Electronic Supplementary Material (ESI) for Journal of Materials Chemistry A.

Supporting Information for

Remarkably enhanced Fenton-like catalytic activity and recyclability of Fe-based metallic glass by alternating magnetic field: mechanisms and industrial applications

Yun-Xuan Ge[1], Peng-Yu Zhu[1], Yao Yu[1], Lai-Chang Zhang[2], Cheng Zhang[1,*] and Lin Liu[1,*]

[1]State Key Laboratory of Materials Processing and Die & Mold Technology, School of Materials Science and Engineering, Huazhong University of Science and Technology, Wuhan 430074, China

[2]School of Engineering, Edith Cowan University, 270 Joondalup Drive, Joondalup, Perth, WA 6027, Australia
*Corresponding authors:

Email: Cheng Zhang (czhang@hust.edu.cn) and Lin Liu (lliu2000@mail.hust.edu.cn)

This PDF file includes:

Supporting text
Figures S1 to S10
Tables S1 to S2
SI References

Other supporting materials for this manuscript include the following:

Movies S1 to S3.

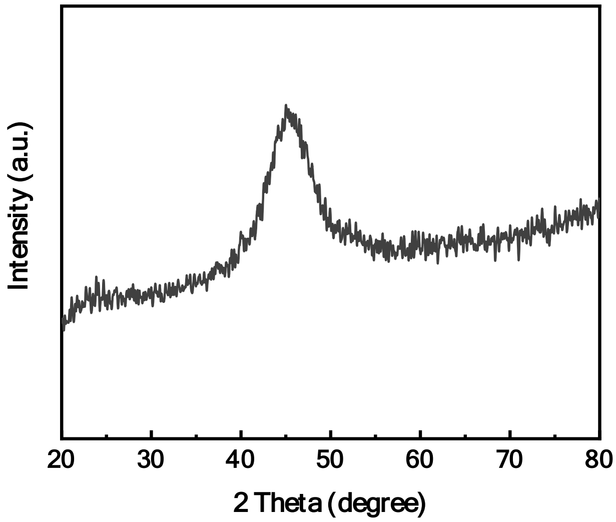

Figure S1. X-ray diffraction (XRD) pattern of the as-received $Fe_{78}Si_9B_{13}$ amorphous ribbon

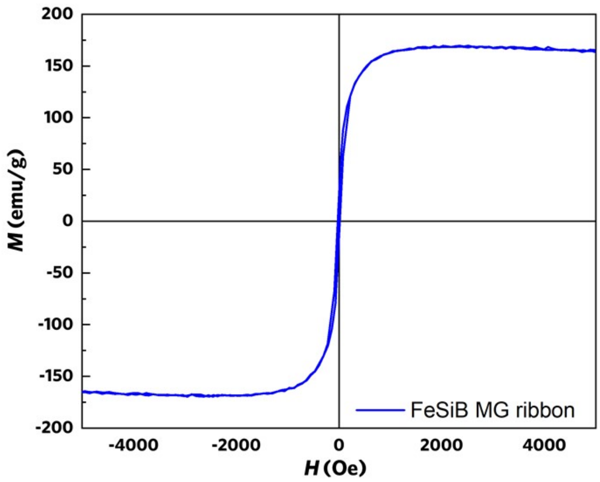

Figure S2. Hysteresis loop of the as-received $Fe_{78}Si_9B_{13}$ amorphous ribbon measured with a vibrating sample magnetometer (VSM), showing the saturation magnetization process

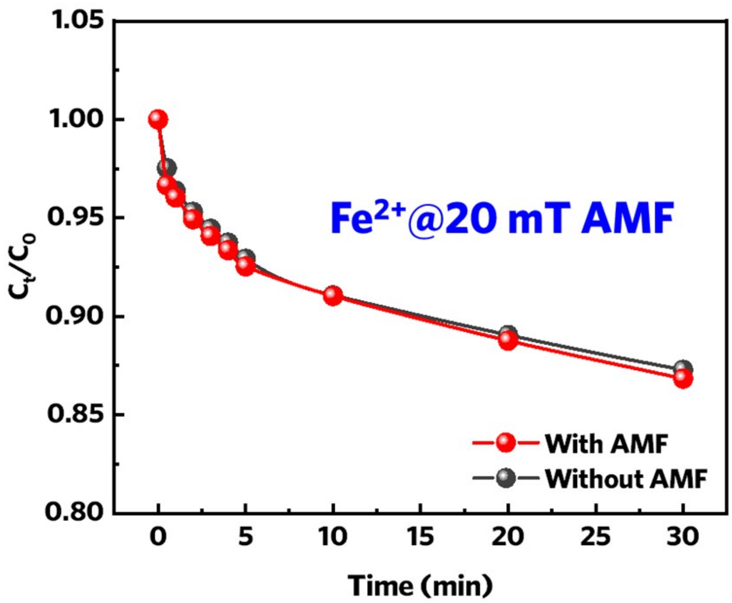

Figure S3. Effect of AMF on the degradation performance of a Fenton system (0.81 mg/L Fe^{2+} ion and 5 mM H_2O_2). (RhB concentration: 10 mg/L; Initial reaction temperature: 302 K; pH=3; *B*=20 mT).

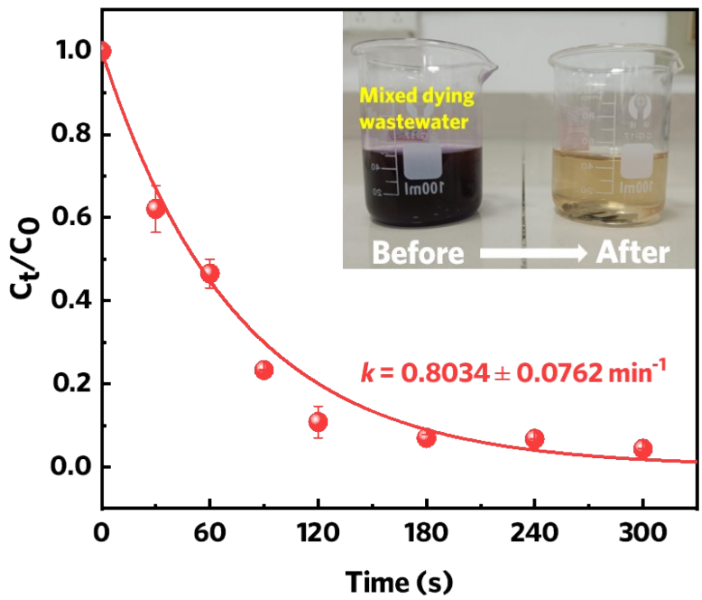

Figure S4. Removal rate of a mixed dye (RhB, methyl orange, methyl blue (MB), methylene blue and brilliant red 3BA) by the FeSiB MG under AMF with a magnetic strength of 20.11 mT.

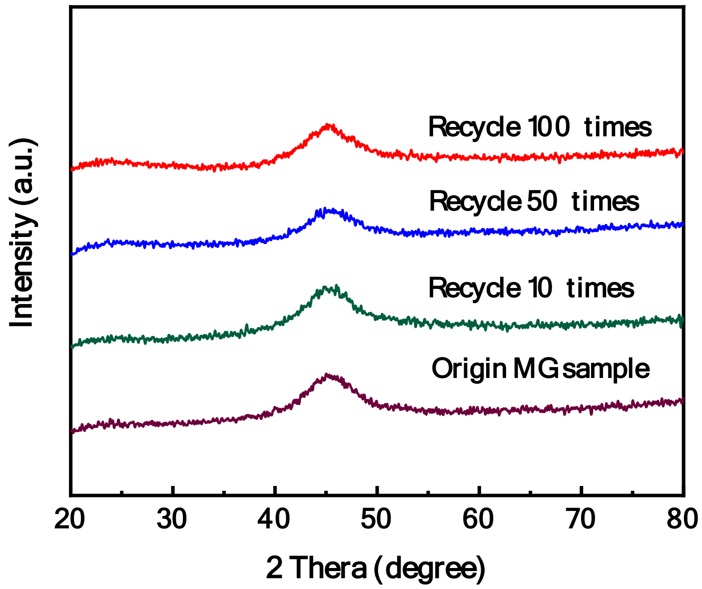

Figure S5. XRD patterns of the FeSiB MG ribbon after reused for various cycle numbers with AMF.

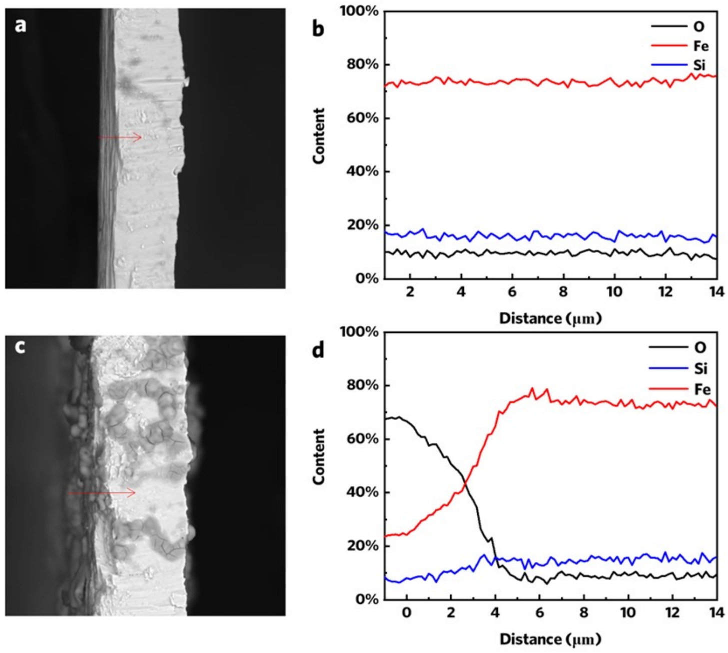

Figure S6. a-b) Cross-section morphology and EDX line scanning on the 100^{th}-reused FeSiB MG ribbon with AMF; c-d) Cross-section morphology and EDX line scanning on the 10^{th}-reused FeSiB MG ribbon without AMF.

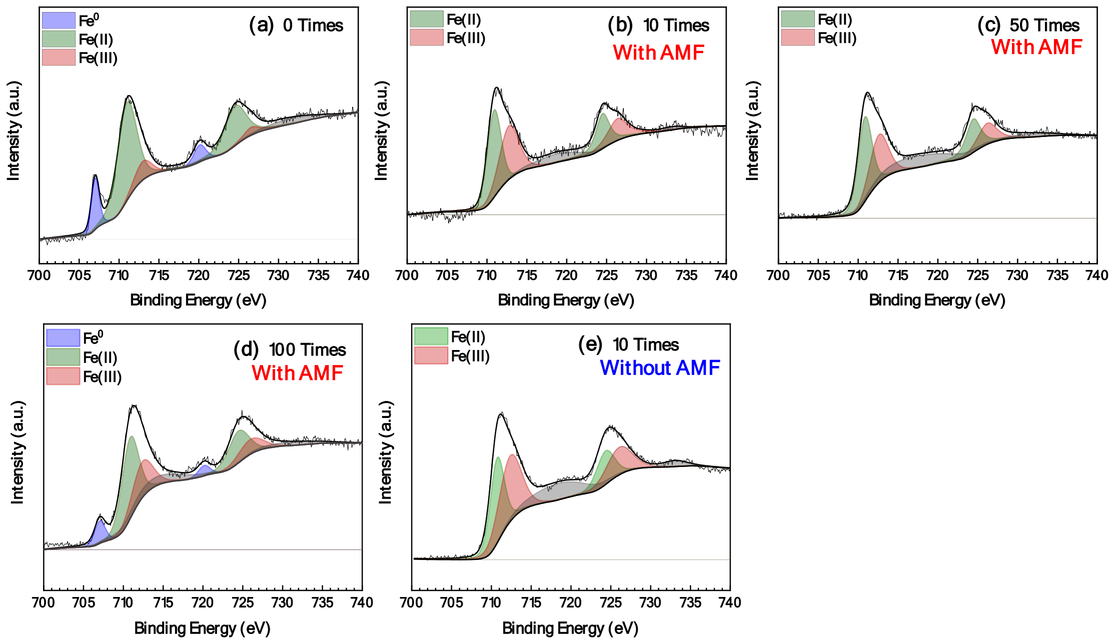

Figure S7. XPS spectra of Fe 2p of the fresh and reused FeSiB MG ribbon after the different reuse times with and without AMF. a) fresh sample; b) the 10th reused sample with AMF; c) the 50th reused sample with AMF; d) the 100th reused sample with AMF; and e) the 10th reused sample without AMF.

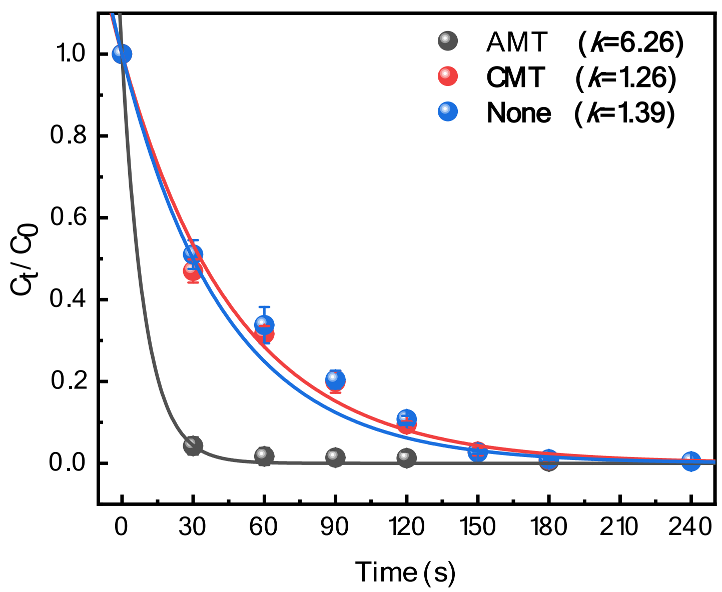

Figure S8. Removal rate of rhodamine B (RhB) by $Fe_{78}Si_9B_{13}$ MG catalysts under alternating magnetic field (AMT, B_{max}=20.11 mT) and constant magnetic field (CMT, B=20.11 mT), compared with that without applying external field. (RhB concentration: 10 mg/L; H_2O_2 concentration: 5 mM; Initial reaction temperature: 302 K; pH=3).

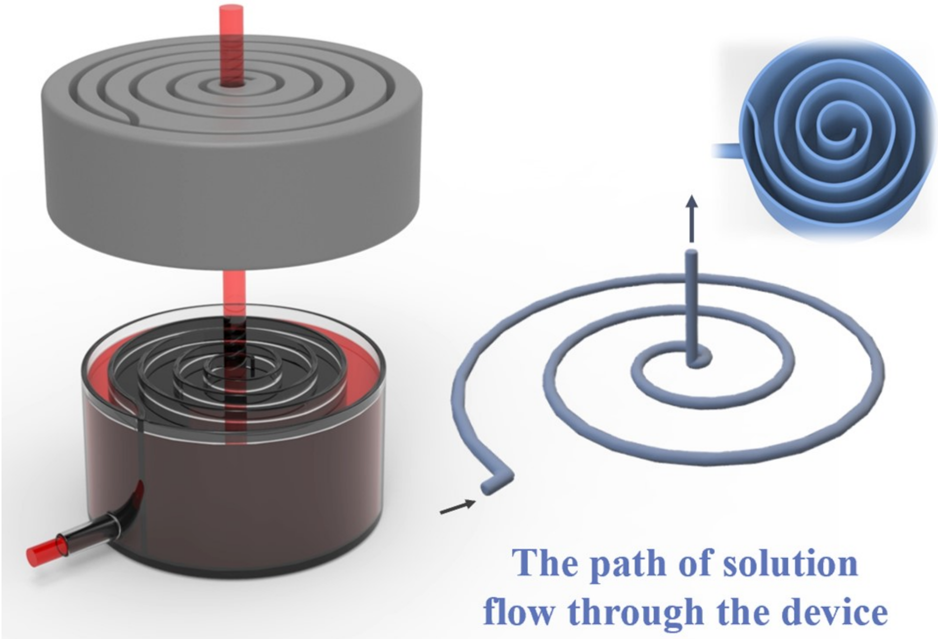

Figure S9. Schematic diagram of the flow-through wastewater treatment device, showing how the water flow in this device.

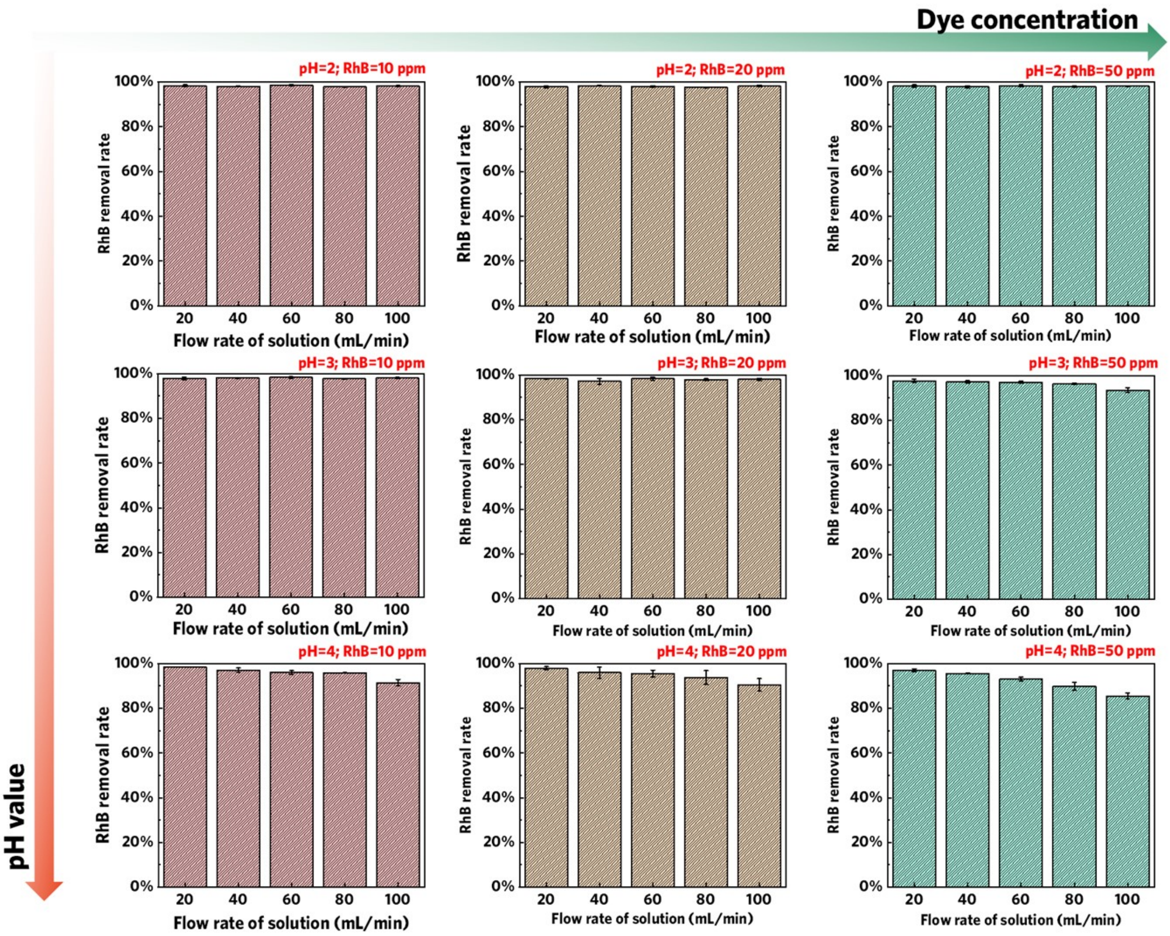

Figure S10. Effects of dye concentration, pH value and flow velocity on the degradation efficiency of RhB under a 20 mT AMF. d) Performance in continuous treatment of RhB under AMF.

Table S1. Comparison of catalytic activity and reusability of Fe-based amorphous and crystalline Fenton-type catalysts.

Catalysts	Organic pollutants	Concentration (ppm)	Area dosage ($m^2 L^{-1}$)[a]	K_{SA} ($L m^{-2} min^{-1}$)[b]	K_{obs} (min^{-1})	Recyclability (times)	Refs.
Metallic glasses							
$Fe_{78}Si_9B_{13}$	Methyl Orannge	20	0.06	6.43	0.386	4	1
	Rhodamine B	20	0.99	7.32	0.725	4	2
	Methyl Blue	20	0.06	6.35	0.381	4	1
	Methyl Blue	20	0.06	5.93	0.356	4	3
	Methylene Blue	20	0.06	10.67	0.64	20	4
	Brilliant Red 3BA	20	0.06	6.2	0.372	4	3
	Brilliant Red 3BA	50	0.26	2.52	0.654	4	5
	Brilliant yellow 3GP	20	0.06	7.76	0.466	4	3
	Malachite Green	20	0.06	8.65	0.519	4	3
	Orange II	200	-	-	0.32	7	6
$Fe_{79}Si_5B_{16}$	Orange G	100	0.005	0.8	0.004	8	7
$Fe_{78}Si_8B_{14}$	Orange II	200	0.83	3.03	0.252	4	7
$Fe_{80}P_{13}C_7$	Methyl Blue	100	-	-	0.56	19	9
$Fe_{76}B_{12}Si_9Y_3$	Methyl Blue	20	-	-	-	13	10
$Fe_{78}(Si, B)_{22}$	Acid Orange II	100	0.062	2	0.125	-	11
$Fe_{73.5}Si_{13.5}B_9Cu_1Nb_3$	Methyl Orannge	20	0.06	2.52	0.152	4	1
	Methyl Blue	20	0.06	3.35	0.201	4	1
	Eosin Y	100	0.099	1.85	0.183	10	12
	Malachite Green	20	0.099	1.64	0.162	5	13

$Fe_{66.3}B_{16.6}Y_{17.1}$	Orange G	100	0.099	9.4	0.011	11	7
$Fe_{83}Si_2B_{11}P_3C_1$	Rhodamine B	20	0.005	45	0.09	35	14
$Fe_{63}Cr_5Nb_4Y_6B_{22}$	Methyl Blue	100	0.002	-	0.182	3	15
$Fe_{50}Ni_{30}P_{13}C_7$	Brilliant Black BN	20	-	1.77	0.175	1	16
$Fe_{81}Si_2B_{10}P_6Cu_1$	Methylene Blue	100	0.396	44.95	1.78	20	17
$Cu_{47.5}Zr_{46}Al_{6.5}$	Acid Orange II	100	0.1	1.65	0.165	10	18
$Cu_{46}Zr_{44.5}Al_{7.5}Gd_2$	Acid Orange II	100	-	-	0.48	80	19
Iron inos							
Fe^{2+}	Rhodamine B	-	-	-	0.12	1	20
	Rhodamine B	-	-	-	2.22	1	20
Zero valent metal							
nZVI	Methyl Orannge	50	23.2	0.022	0.56	1	21
Micro-ZVI	Acid Orange II	105	1.42	0.27	0.38	-	22
FeCo	Acid Orange II	105.1	2134.8	$1.2*10^{-5}$	0.025	4	23
FeCu/CNF	Orange II	100	133	$4.3*10^{-5}$	0.057	5	24
Minerals							
Fe(II)/Hematite NP	Rhodamine B	5	83.6	0.0004	0.033	5	25
Graphite tailings	Rhodamine B	100	497	$1.6*10^{-4}$	0.077	1	26
Fe-Oixdes							
$BiFeO_3$	Rhodamine B	4.79	4.17	0.007	0.0289	5	27
Fe_2O_3/FCNT	Methyl Blue	8	8.24	0.006	0.053	5	28
Fe_3O_4	Rhodamine B	10	0.003	6.33	0.019	6	29
Fe_3O_4/MIL-101	Rhodamine B	10	16858.9	$9.23*10^{-6}$	0.164	5	30
Fe_3O_4	Rhodamine B	4.79	1152	$2.44*10^{-5}$	0.0281	6	31
Single-atom catalyst							

Fe-g-C_3N_4/GMC	Rhodamine B	50	3705	5.64*10^{-5}	0.209	7	32
Metal phosphides							
Fe^{2+}/FeP	Methylene Blue	100	12.16	1.2*10^{-4}	0.0015	7	32
Cu_3P	Sulfamethoxazole	0.5	0.32	0.625	0.20	1	33
Co_2P/C compsites	Bisphenol A	22.8	6.28	0.42	2.644	5	34
3D-printed MGs							
$Fe_{70}Cr_5Ni_3Mo_3W_9Si_5B_5$	Brilliant Red 3BA	20	-	-	0.586	45	35
$Fe_{68}Cr_2Ni_5Mo_5P_{12.5}$ $C_5B_{2.5}$/Cu	Rhodamine B	20	0.019	34.3	0.64	73	36
Re-activated $Fe_{68}Cr_2Ni_5Mo_5P_{12.5}$ $C_5B_{2.5}$/Cu	Rhodamine B	20	0.019	43	0.83	100	36
This work							
$Fe_{78}Si_9B_{13}$ with AMF	Rhodamine B	10	0.04	157.5	6.3	100	**This Work**
$Fe_{78}Si_9B_{13}$ without AMF	Rhodamine B	10	0.04	33.38	1.34	15	

Table S2. EIS fitting results under AMF and without AMF.

B (mT)	R_s (Ωcm²)	R_f (Ωcm²)	R_{ct} (Ωcm²)	CPE_1 (μΩ^{-1}cm^{-2}S^n)	n_1	CPE_{dl} (μΩ^{-1}cm^{-2}S^n)	n_{dl}	C_{dl} (μF cm^{-2})	d_{eff} (nm)
0	73.28±0.53	51.96±0.03	96.76±1.10	74.68±1.43	0.79±0.01	13.6±0.08	0.82±0.01	2.63±0.04	5.26
5	72.64±0.19	34.46±0.05	80.56±0.93	43.06±0.50	0.81±0.01	16.25±0.11	0.83±0.01	3.42±0.05	4.04
10	69.55±0.87	32.65±0.01	76.45±1.59	44.65±0.36	0.83±0.01	16.12±0.22	0.83±0.01	3.51±0.04	3.94
20	66.55±0.37	30.78±0.03	70.62±0.87	41.95±0.42	0.83±0.01	16.04±0.09	0.83±0.01	3.47±0.07	3.98

Supplementary References

[1] Jia, Z.; Kang, J.; Zhang, W.C.; Wang, M.; Yang, C.; Sun, H.; Habibi, D.; Zhang, L.C. Surface Aging Behavior of Fe-Based Amorphous Alloys as Catalysts During Heterogeneous Photo Fenton-Like Process for Water Treatment. *Appl. Catal. B: Environ.* **2017**, 204, 537-547.

[2] Wang, X.; Pan, Y.; Zhu, Z.; Wu, J. Efficient Degradation of Rhodamine B Using Fe-Based Metallic Glass Catalyst by Fenton-Like Process. *Chemosphere*, **2014**, 117, 638-643.

[3] Jia, Z.; Duan, X.; Qin, P.; Zhang, W.; Wang, W.; Yang, C.; Sun, H.; Wang, S.; Zhang, L-C. Disordered Atomic Packing Structure of Metallic Glass: Toward Ultrafast Hydroxyl Radicals Production Rate and Strong Electron Transfer Ability in Catalytic Performance. *Adv. Funct. Mater.*, **2017**, 27, 1702258.

[4] Jia, Z.; Duan, X.; Zhang, W.; Wang, W.; Sun, H.; Wang, S.; Zhang, L.-C. Ultra-Sustainable Fe78si9b13 Metallic Glass as a Catalyst for Activation of Persulfate on Methylene Blue Degradation under Uv-Vis Light. *Sci Rep*, **2016,** 6, 38520.

[5] Jia, Z.; Zhang, W.C.; Wang, W.M.; Habibi, D.; Zhang, L.C. Amorphous $Fe_{78}Si_9B_{13}$ Alloy: An Efficient and Reusable Photo-Enhanced Fenton-Like Catalyst in Degradation of Cibacron Brilliant Red 3b-a Dye under UV–Vis Light. *Appl. Catal. B: Environ.* **2016**, 192, 46-56.

[6] Qin, X.; Li, Z.; Zhu, Z.; et al. Mechanism and Kinetics of Treatment of Acid Orange II by Aged Fe-Si-B Metallic Glass Powders. *J. Mater. Sci. Technol.*, **2017**, 33, 1147-1152.

[7] Liu, P., Zhang, J.L.; Zha, M.Q.; Chek, C.H. Synthesis of an Fe Rich Amorphous Structure with a Catalytic Effect to Rapidly Decolorize Azo Dye at Room Temperature. *ACS Appl Mater Interfaces*, **2014**, 6, 5500-5505.

[8] Zhang, C.; Zhu, Z.; Zhang, H.; Hu, Z. Rapid Decolorization of Acid Orange II Aqueous Solution by Amorphous Zero-Valent Iron. *J. Environ. Sci.*, **2012**, 24, 1021-1026.

[9] Wang, Q.; Chen, M.; Lin, P.; Cui, Z.; Chu, C.; Shen, B. Investigation of FePC Amorphous Alloys with Self-Renewing Behaviour for Highly Efficient Decolorization of Methylene Blue. *J. Mater. Chem. A*, **2018**, 6, 10686-10699.

[10] Xie, S.; Huang, P.; Kruzic, J.J.; Zeng, X.; Qian, H. A Highly Efficient Degradation Mechanism of Methyl Orange Using Fe-Based Metallic Glass Powders. *Sci. Rep.*, **2016**, 6, 21947.

[11] Zhang, C.; Zhu, Z.; Zhang, H.; Hu, Z. Rapid Reductive Degradation of Azo Dyes by a Unique Structure of Amorphous Alloys. *Chin. Sci. Bull.*, **2011**, 56, 3988-3992.

[12] Wang, J.C.; Jia, Z.; Liang, S.X.; Qin, P.; Zhang, W.C.; Wang, W.M.; Sercombe, T.B.; Zhang, L.C. $Fe_{73.5}Si_{13.5}B_9Cu_1Nb_3$ Metallic Glass: Rapid Activation of Peroxymonosulfate Towards Ultrafast Eosin Y Degradation. *Mater. Des.*, **2018**, 140, 73-84.

[13] Liang, S.X.; Jia, Z.; Zhang, W.C.; Zhang, L.C. Rapid Malachite Green Degradation Using $Fe_{73.5}Si_{13.5}B_9Cu_1Nb_3$ Metallic Glass for Activation of Persulfate under Uv–Vis Light. *Mater. Des.*, **2017**,119, 244-253.

[14] Jia, Z.; Wang, Q.; Sun, L.; Wang, Q.; Zhang, L.-C.; Wu, G.; Luan, J.-H.; Jiao, Z-B.; Wang, A.; Liang, S.-X., Gu, M.; Lu, J. Attractive in situ Self-reconstructed Hierarchical Gradient Structure of Metallic Glass for High Efficiency and Remarkable Stability in Catalytic Performance. *Adv. Funct. Mater*. **2019**, 29 1807857.

[15] Yang, W.; Wang, Q.; Li, W.; Xue, L.; Liu, H.; Zhou, J.; Mo, J.; Shen, B.L. A Novel Thermal-Tuning Fe-Based Amorphous Alloy for Automatically Recycled Methylene Blue Degradation. *Mater. Des.*, **2019**, 161, 136-146.

[16] Liang, S-X.; Zhang, W.; Wang, W.; Jia, G.; Yang, W.; Zhang, L.C. Surface Reactivation of Fenipc Metallic Glass: A Strategy for Highly Enhanced Catalytic Behavior. *J Phys. Chem. Solids*, **2019**,132, 89-98.

[17] Wang, Q.; Yun, L.; Chen, M.; Xu, D.; Cui, Z.; Zeng, Q.; Lin, P.; Chu, C.; Shen, B. Competitive Effects of Structural Heterogeneity and Surface Chemical States on Catalytic Efficiency of FeSiBPCu Amorphous and Nanocrystalline Alloys. *ACS Appl. Nano Mater.*, **2019**, 2, 214-227.

[18] Zhao, B.; Zhu, Z.; Qin, X.D.; Li, Z. Zhang, H.F. Highly Efficient and Stable CuZr-based Metallic Glassy Catalysts for Azo Dye Degradation. *J. Mater. Sci. Technol.* **2020**, 46, 88-97,.

[19] Li, Z.; Qin, X.D.; Zhu, Z.; Zheng, S.; Li, H.; Fu, H.; Zhang, H.F. Cu-based Metallic Glass with Robust Activity and Sustainability for Wastewater Treatment. *J Mater. Chem. A* **2020**, 8, 10855-10864.

[20] Xing, M.; Xu, W.; Dong, C.; Bai, Y.; Zeng, J.; Zhou, Y.; Zhang, J.; Yin. Y. Metal Sulfides as Excellent co-catalyst for H2O2 Decomposition in Advanced Oxidation Processes. *Chem*, **2018**, 4, 1359-1372.

[21] Fan, J.; Guo, Y.; Wang, J.; Fan, M. Rapid Decolorization of Azo Dye Methyl Orange in Aqueous Solution by Nanoscale Zerovalent iron Particles. *J. Hazard. Mater.* **2009**, 166, 904-910.

[22] Nam, S.; Tratnyek, P. Reduction of Azo Dyes with Zero-valent Iron. *Water. Res.*, **2000**, 34, 1837-1845.

[23] Ganiyu, S.; Le, T.; Bechelany, M.; Esposito, G.; Hullebusch, E.D.V.; Oturan, M.A.; Cretin, M. A hierarchical CoFe-layered Double Hydroxide Modified Carbon-felt Cathode for Heterogeneous Electro-Fenton Process. *J. Mater. Chem. A*, **2017**, 5, 3655-3666.

[24] Wang, J.; Liu, C.; Li, J.; Luo, R.; Hu, X.; Sun, X.; Shen, J.; Han, W.; Wang, L. In-situ Incorporation of Iron-copper Bimetallic Particles in Electrospun Carbon Nanofibers as an Efficient Fenton Catalyst. *Appl. Catal. B: Environ.*, **2017**, 207, 316-325.

[25] Huang, X.; Hou, X.; Zhao, J.; Zhang, L. Hematite Facet Confined Ferrous ions as High Efficient Fenton Catalysts to Degrade Organic Contaminants by Lower in H_2O_2 decomposition Energetic Span. *Appl. Catal. B: Environ.*, **2016,** 181, 127-137.

[26] Bai, C.P.; Gong, W.; Feng, D.; Mo, X.，Qi, Z. Natural Graphite Tailings as Heterogeneous Fenton Catalyst for the Decolorization of Rhodamine B. *Chem. Eng. J.*, **2012**, 197, 306.

[27] Luo, W.; Zhu, L.; Wang, N.; Tang, H.; Cao, M.; She, Y. Efficient Removal of Organic Pollutants with Magnetic Nanoscaled $BiFeO_3$ as a Reusable Heterogeneous Fenton-like Catalyst. *Environ. Sci. Technol.*, **2010**, 44, 1789-1791.

[28] Yang, Z.; Qian, J.; Yu, A.; Pan, B. Singlet Oxygen Mediated Iron-based Fenton-like Catalysis under Nanoconfinement. *Proc Natl Acad Sci USA*, **2019**, 116, 6659-6664.

[29] Nidheesh, P.; Gandhimathi, R.; Velmathi, S.; Sanjini, N.S. Magnetite as a Heterogeneous Electro Fenton Catalyst for the Removal of Rhodamine B from Aqueous Solution. *RSC Adv.*, **2014**, 4, 5698-5708.

[30] Zhao, C.; Dong, P.; Liu, Z.; Wu, G.; Wang, S.; Wang, Y.; Liu, F. Facile Synthesis of Fe_3O_4/MIL-101 Nanocomposite as an Efficient Heterogeneous Catalyst for Degradation of Pollutants in Fenton-like System. *RSC Adv.*, **2017**, 7, 24453-24461.

[31] Chen, F.; Xie, S.; Huang, X.; Qiu, X. Ionothermal Synthesis of Fe_3O_4 Magnetic Nanoparticles as Efficient Heterogeneous Fenton-like Catalysts for Degradation of Organic Pollutants with H_2O_2. *J. Hazard. Mater.*, **2017**, 322, 152-162.

[32] Ma, J.; Yang, Q.; Wen, Y.; Liu, W. Fe-g-C_3N_4/Graphitized Mesoporous Carbon Composite as Effective Fenton-like Catalyst in Wide pH Range., *Appl. Catal. B: Environ.*, **2017**, 201, 232-240.

[33] Ma, C.; Feng, S.; Zhou, J.; Chen, R.; Wang, S. Enhancement of H_2O_2 Decomposition Efficiency by the co-catalytic Effect of Iron Phosphide on the Fenton Reaction for the Degradation of Methylene Blue. *Appl. Catal. B: Environ*, **2019**, 259, 118015.

[34] Alexopoulou, C.; Petala, A.; Frontistis, Z.; Drivas, C.; Kennou, S.; Kondarides, D.I.; Mantzavinos, D. Copper Phosphide and Persulfate Salt: A Novel Catalytic System for Degradation of Aqueous Phase Micro-contaminants. *Appl. Catal. B: Environ*, **2019**, 244, 178.

[35] Liang, S.H.; Wang, X.; Zhang, W.; Liu, Y.-J.; Wang, W.; Zhang, L-C. Selective Laser Melting Manufactured Porous Fe-based Metallic Glass Matrix Composite with Remarkable Catalytic Activity and Reusability. *Appl. Mater. Today*, **2020**, 19, 100543.

[36] Tong, W.; Xie, Y.; Luo, H.Q.; Niu, J.; Ran, W. Phosphorous-Rich Microorganism-Enabled Synthesis of Cobalt Phosphide/Carbon Composite for Bisphenol A Degradation Through Activation of Peroxymonosulfate. *Chem. Eng. J.*, **2019**, 378, 122187.